

Article

An Adaptive Beamforming Time with Round-Robin MAC Algorithm for Reducing Energy Consumption in MANET

Vincenzo Inzillo ^{1,*} , Floriano De Rango ¹, Alfonso A. Quintana ² and Amilcare F. Santamaria ¹

¹ DIMES, University of Calabria, 87036 Rende, Italy; derango@dimes.unical.it (F.D.R.); af.santamaria@dimes.unical.it (A.F.S.)

² Department of Electronic Technologies, University of Malaga, 29007 Malaga, Spain; aarizaq@uma.es

* Correspondence: v.inzillo@dimes.unical.it

Received: 23 October 2018; Accepted: 19 November 2018; Published: 23 November 2018



Abstract: The use of smart antenna systems (SASs) in mobile ad hoc networks (MANETs) has been promoted as the best choice to improve spatial division multiple access (SDMA) and throughput. Although directional communications are expected to provide great advantages in terms of network performance, directional MAC (medium access control) protocols introduce several issues. One of the most known problems in this context is represented by the fact that, when attempting to solve or at least mitigate the problems introduced by these kinds of antennas especially at MAC layer, a large amount of energy consumption is achieved; for example, due to excessive retransmissions introduced by very frequently issue such as deafness and handoff. The expedients proposed in order to reduce these drawbacks attempting to limit beamforming time of nodes in cooperation with a round-robin scheduling can grant high performance in terms of fairness and throughput. However, the overall energy distribution in the network is not efficient due to static approach. In view of this, we propose adaptive beamforming time with round-robin MAC providing a dynamic assignment of the beamforming time with the aim to limit the waste of energy of nodes. The proposed approach provides benefits in terms of energy consumption distribution among nodes in sectorized antennas environments and, simultaneously, improves MAC packet performance.

Keywords: beamforming; energy consumption; MAC, MANET, round-robin; SAS

1. Introduction

In the latest research studies, relating to wireless network environments, one of the most significant and, at the same time, critical issues is represented by the management of energy consumption of nodes that could highly limit the overall network performance with reference to protocols and application fields. In this regard, several aspects should be considered in order to address the problems implied by the main features of these kinds of networks that significantly affect the behaviors at physical, MAC, and network layers. For instance, let us consider mobile ad hoc networks (MANETs); usually, in these kinds of environments, omnidirectional antennas are used for communication among nodes both for transmission as well as for reception; this approach results in very limited performance relating to physical, link, and routing layer statistics [1–4]. Omnidirectional antennas have the ability to transmit and receive signals in the same way in all directions. Main advantages of omnidirectional antennas include ease of configuration and implementation, low designing cost, very and simple architecture (hardware-less) [5,6]. Nevertheless, despite these few benefits they introduce a considerable number of drawbacks such as limited range and coverage (implied by low gain), high energy consumption, high interference probability (especially in dense networks),

and very high performance dependency on the environments in which they are employed (indoor or outdoor) [7,8]; nonetheless, omnidirectional antennas cannot exploit the benefits of cross-polarization because they are vertically polarized [9]. More specifically, this last issue helps to increase the probability of interference between communicating nodes in the channel [10]. The majority of these issues could be partially mitigated using directional antennas. Directional antennas offer a great number of benefits with respect to the classic omnidirectional antennas. In fact, because they focus the radiating power only toward a specific direction, directional antennas are able to improve the spatial reuse as well as the coverage range of the signal. Higher spatial reuse and longer communication range is reflected in greater network capacity and improved network connectivity [11–13]. Most researchers, as we presented in Section 2, in order to mitigate these undesired phenomena in directional contexts, demonstrated that, through the employment of smart antenna systems (SASs) in place of the classic directional antennas, it is possible to create an efficient system, exploiting the Spatial Division Multiplexing (SDMA) technique that this kind of device well provides. Using an SAS, efficient spatial reusing and high link robustness may be obtained [14,15]. In contexts in which directional smart antenna systems are used, the beamforming issue has to be deeply investigated. The use of DRTS and DCTS messages along with directional network allocator vector (DNAV) aims to reduce the excessive burden of collisions occurring when omnidirectional antennas are used; however, when SASs are employed, it is not sufficient to adopt these expedients [16–19]. The most common drawback in this field is represented by the fact that, in literature, there is an important lack relating to directional MAC proposals that could be synthesized by two main aspects: Primarily, most directional MAC works are designed for classical directional antennas and do not address issues involved by the use of an SAS. This aspect represents a huge limit for latest wireless mobile network developments that, however, allow for the use of more complex antennas technologies such as SASs and massive MIMO systems. Secondly, addressing directional MAC and, at the same time, energy consumption issues when using SAS technologies represents a very critical task; indeed, in case of high gain directive communication beams, it is hard to limit the overall waste of energy of nodes, precisely because it is an implication induced by the employment of high gains. Unfortunately, in order to meet energy efficiency requirements in directional high gain communications, it is not sufficient to consider to limit the most important source of waste of energy that is related to hardware resources, because issues introduced by directional communications are prone to degrade the battery life duration of mobile nodes and hardware operations [20,21]; in particular, in sectorized antennas environments, it should be advisable to control the maximum number of communications performed by nodes or to reduce beamforming time, especially in data traffic exchange [22]. In view of these considerations, in the present paper, we propose addressing the energy consumption issue by enhancing the works proposed in [23,24] using SASs along with a round-robin scheduling. The main purpose of the work is to limit the excessive energy consumption in the network derived by the queue and the time slice problems involved by the use of the round-robin. The other goal is to demonstrate how, using a mechanism enhancing the channel resources exploitation, could lead to MAC performance improvement especially in terms of packet delivery ratio (PDR).

2. Related Works

Relating to MAC layer communications, most causes of excessive energy consumption in mobile network scenarios include the use of omnidirectional antennas, data processing, high protocol overhead, and a high level of interference in the channel. Data processing implies the large usage of a central processing unit (CPU), memory, hard drive, etc. To partially solve this issue, regarding energy consumption, the most actual solution is to find a compromise between data processing and radio communication [21]. In this regard, in [20], the authors present a data compression mechanism in order to minimize packet length with the aim to limit energy consumption in radio communication. In [25], the authors highlight the large protocol overhead introduced by this kind of system. Generally, to design an energy efficient MAC protocol, some of the following expedients are employed:

- **Reducing collisions and retransmissions:** This is one of the most common objective of MAC protocols for limiting the probability of interfering nodes. In this context, the work [26] proposes a novel deafness-aware (DA-MAC), with the goal to mitigate the deafness problem through a discrete-time Markov chain model. The model uses a double-channel schema in order to handle the directional RTS (DRTS); more specifically, the single channel provided by the directional MAC is split into two different logical channels used for filtering the data traffic and the control packets, respectively; the designed DA-MAC algorithm provides for several features that allows one to recognize and mitigate efficiently the collisions occurred because of deafness. The results highlight a reduction of the deafness duration and a good improvement of the aggregate throughput compared with some of the most significant existing works.
- **Reducing overhearing:** Wireless mobile nodes deplete battery life also because they overhear transmissions of their neighbors. One possible solution to mitigate this problem is to use dedicated and separated channel distinguishing control and data traffic so that nodes do not overhear undesired information. For example, the authors in [27] propose a schedule-based broadcast mechanism including data transmission timers for each node. In [28], two schemes are proposed in order to mitigate the deafness caused by persistent hearing of data and for handling the short retry limit (SRL) in directional environments.
- **Minimize control overhead:** Limiting the protocol overhead represents a critical challenge, especially when small packets are used [29–31]. Because of the important channel acquisition overhead, the high amount of small packets to be transmitted translates into a significant waste of energy. However, if mobile nodes perform multiple transmission slot requests with a single reservation message, the control overhead can be limited [32]. In [22], the authors propose two MAC protocols in which nodes use directional sectorized antennas. The scheduler and the protocols are designed with the aim to minimize the co-site interference issue that could arise in some directional contexts also by limiting the overall overhead in the network.
- **Reducing beamforming time:** In [3], the authors propose a tone DMAC mechanism that enable the transmission of special packets (out-of band tones) by nodes in omnidirectional mode; these tones can be processed by neighbors reducing considerably the large backoff time introduced by deafness. In [24], a round-robin MAC (RR-MAC) approach is presented with the goal to minimize the impact of deafness in directional MAC contexts. The round-robin mechanism was implemented by an algorithm that manages the assignment of the beam toward a certain sector also handling the incoming frames that could not temporally be transmitted in the channel by using waiting queues.

The RR-MAC (Figure 1) allows for the communication plane to be divided into identical sectors, each of them having a certain amplitude w (sector width) and a beamforming duration time T_i (sector time). More specifically, all sectors have equal width and sector time; in each sector, nodes attempt communications by beamforming toward the intended receiver with an angle α_i for the entire duration of the sector time; the systems operates in a circular way by enabling (for communications) one sector at a time; the sector in which the beamforming is currently enabled is denoted as *current active sector*.

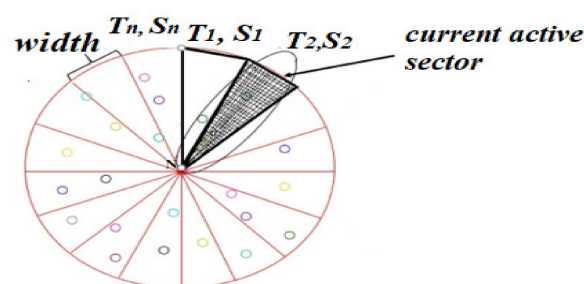


Figure 1. Round-robin MAC principle.

A non-negligible matter in directional MAC contexts is certainly represented by the handoff problem that involves the mobility of nodes. For example, in [33], the authors attempt to limit the handoff problem through the use of an efficient beam control mechanism; a similar approach is proposed in [34] in which handoff is reduced using a predictive location model that is able to estimate future movements of nodes. Similarly, the work [35] presents a predictive location algorithm using in-frame priority scheduling in order to reduce the handoff.

3. Omnidirectional and Directional Antennas Issues vs. Round-Robin MAC

3.1. Directional Antennas in MANET Common Issues

As mentioned in the introduction section, using directional antennas in MANET communications in place of the classic omnidirectional systems implies several advantages. In order to understand the reasons for employing directional antennas, the following example scenario is considered:

Figure 2 illustrates a wireless network scenario in which nodes use omnidirectional antennas to perform communications. In particular, the transmitter node T sends to the receiver R a communication signal by using an omnidirectional antenna; R attempts to capture the signal with the same antenna model. Because the transmitter signal is radiated in all directions with the same intensity, if there are such nodes in the neighboring of the transmitter/receiver (N_T and N_R), it is possible that the radiated signal is captured by these nodes that, in turn, may attempt a communication at the same time. In this case, interferences and collisions can occur [36–38]; these issues could enhance with increasing mobility of nodes. Nevertheless, in this case, because nodes radiate in the same way toward all directions, a huge waste of the battery life of nodes is certainly achieved [39,40]. In any case, several issues have to be addressed in the case of directional communications among nodes in MANET; the most common include hidden terminal and deafness problems.

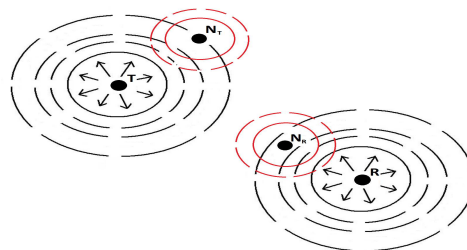


Figure 2. Interference caused by omnidirectional antennas.

Referring to directional MAC communications in which directional request-to-send (DRTS) and directional clear-to-send (DCTS) are used to perform a transmission/reception flow, it is possible that a special node (denoted by deaf node) that is engaged in a certain communication, but at the same time is solicited as a receiver by another source node, causes the deafness problem (Figure 3a). The node that experiences the deafness (the node A in Figure 3a) could try to retransmit many times MAC layer packets, resulting in a large amount of collisions and a considerable increase of the network overhead. In any case, due to recurring retransmissions attempted by the deaf node, a significant waste of energy could occur, and in turn this node tends to deplete its battery life quickly; as a consequence, the overall network throughput is subject to an important degradation. Another common issue while using directional antennas is represented by the handoff problem that is usually implied by the movements of nodes in the network. In Figure 3b, the handoff issue is depicted: the sender node T beamforms a communication toward a receiver R ; when the communication is still active, R shifts in the position R' getting out of the transmitter beam; as a result, the ongoing communication fails and beams have to be re-pointed. If a proper mechanism of synchronization and node position refreshing is not provided, the directional beam remains tuned for a long time in an undesired direction due to node movement; for this reason, again, a great amount of energy consumption occurs.

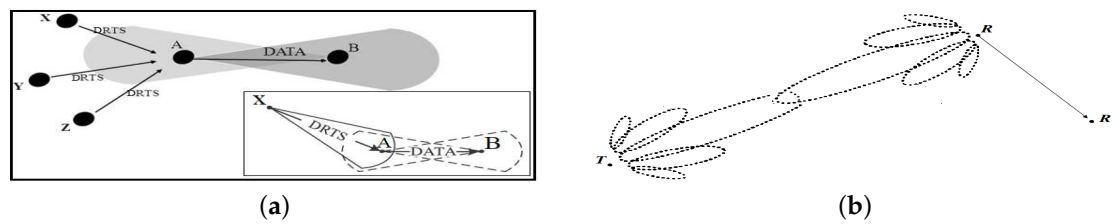


Figure 3. Directional antennas common issues in mobile ad hoc networks (MANETs). (a) Deafness problem. (b) Handoff problem.

3.2. Round-Robin MAC Scheduling Issues

As largely mentioned in the previous sections, networks containing nodes equipped with omnidirectional antennas are prone to a high waste of energy because the shape of the radiation pattern that does not beamform is only in a specific direction. Although different proposals exist with the aim to solve or at least mitigate the issues derived from the use of omnidirectional and directional antennas at the MAC layer, a deeper analysis is required for highlighting the issues that need to be addressed. For example, let us consider the work [24] that attempts to mitigate the overall network energy consumption using an SAS antenna module along with a round-robin scheduler algorithm. Basically, it works fine under two main assumptions:

Assumption 1. Nodes are equipped with high-efficient hardware antennas (SAS).

Assumption 2. Data traffic and nodes are uniformly distributed among sectors.

Assumption 3. The size of the sector queues are fixed and equals for all sectors.

In order to evaluate the implications of the first assumption, it can be useful to analyze the behavior of the RR-MAC in case the omnidirectional antenna is used in place of directional or SAS technologies. For this purpose, we evaluate, through the use of the *Omnet++* network simulator [41], the energy consumption of nodes of three different run configurations using the same simulation parameters described in [24] (most of the them are illustrated in Table 1 in Section 5 of the present paper); in order to accomplish the analysis, energy simulation modules have been provided for each node. Nodes are initially charged with an energy amount of 300 J; a node turns off when it reaches an energy value of 0 J. In the first configuration run nodes are equipped with the classical omnidirectional antenna; in the second, nodes use the omnidirectional antenna together with the RR-MAC scheduling; the latest run configuration is similar to the second except from the fact that in this case the antenna is the SAS module designed in [42].

Table 1. Main simulation parameter set.

Parameter	Value
SAS Array Elements Spacing	0.5 λ
Steering Angle	45°
Transmission Rate	54 Mbps
Message Length	512 Byte
Mobility Model	Random Waypoint
Node Mobility speed	from 1 to 10 mps
Routing Protocol	AODV
Network Load	50%
Simulation Area Size	500 m \times 500 m
Simulation Time	300 s
Number of Sectors	3, 4, 6, 8
Initial Battery Capacity	300 J

Figure 4 depicts the residual capacity (averaged by all nodes) plot comparison between the three considered cases. As we can expect, when using the omnidirectional antenna without any energy saving mechanism, nodes deplete their battery life very quickly; when the omnidirectional antennas are used in cooperation with RR-MAC the average depletion time is almost doubled ($t = 190$ s) and improves significantly when SASs are employed by nodes. This is mainly due to the fact that RR-MAC limits the beamforming time for each sector translating into a reduction of the number collisions and interferences. The mentioned assumptions imply that the system could be affected from the queue size and the waiting queue time problems [43] that can affect the overall network consumption in the network. We analyze these issues by creating two more run configurations: in the first one, mobile nodes are uniformly placed in the network; in the same way, the activity degree of nodes is uniformly distributed among sectors; in the second, instead, nodes are periodically concentrated in a certain sector (randomly chosen) of the sectorized plane and the activity degree of nodes is unbalanced among sectors. The number of sectors in the plane varies from 3 to 8, while the queue size is evaluated based on the following equation:

$$Queue\ size = Q \times [N + w_Q(N_s)] \quad w_Q \in \overline{W}_Q. \tag{1}$$

The queue size is a function of N that is the number of nodes in the network, and N_s denotes the number of sectors in the plane. Q is a value chosen in the interval $0.1 \leq Q \leq 0.25$ in order to maximize the packet delivery ratio performance of [24]. The number of sectors is weighted by the term w_Q , which varies from 1 to 6 as the sector number value increases. In particular, given the sector number array $\overline{S} = [3, 4, 5, 6, 7, 8]$, the weight vector \overline{W}_Q is expressed by

$$\overline{W}_Q = [1, 2, 3, 4, 5, 6]. \tag{2}$$

In order to verify the impact of the two simulation scenarios relating to the queue issues, we compare the waiting queue time of the two running configurations in function of the number of sectors and queue size.

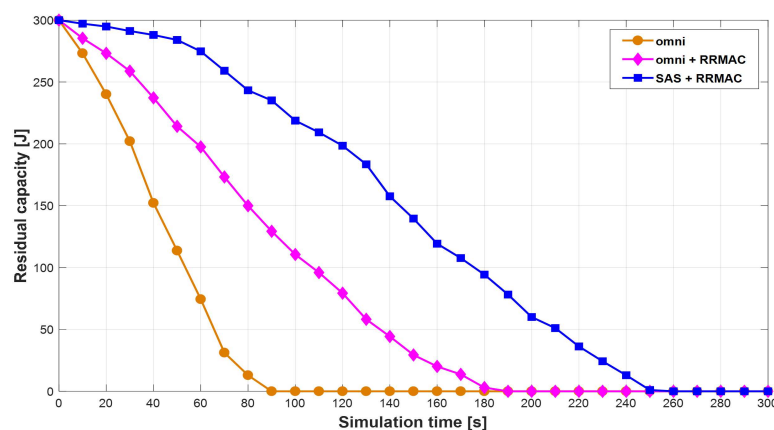


Figure 4. Residual capacity progression.

Figure 5 illustrates the average waiting queue time in function of the number of sectors. The waiting queue time is averaged by varying the Q parameter from 0.1 to 0.25. In Figure 5a, it can be highlighted that the waiting queue time in the case of non-uniform distributed nodes remains higher than the uniform case independently from the sector number value; in particular, the gap between the waiting queue time of the two considered cases seeks to grow for sector number values higher than 5. The curves of Figure 5b are plotted in function of the Q parameter, which represents a proper index of the queue size; as can be deduced from Equation (1), the higher the Q value is, the higher the queue size is. As shown in Figure 5a, the waiting queue time in the case of non-uniform

traffic lies above the uniform case curve independently from the queue size. However, as opposed to Figure 5a, the difference between curves has remained almost constant as the queue size increases. In the uniform traffic case, it can be noted how the waiting time slightly decreases for the highest values of Q , while, in the non-uniform case, the decrease corresponding to the same values is closely negligible. In summary, as the size of the queue increases, the waiting time in the non-uniform case does not tend to decrease, or rather, the decreasing related to high queue size values is not significant. The trends evaluated in Figure 5 are certainly justified by one of the most common issues implied by a round-robin algorithm scheduling: the time slice problem [44,45]; basically, the time slice represents the quantum assigned to each sector (the sector time) in equal portions; therefore, the communications are handled in a circular way among sectors without priority. In the case of non-uniform distributed traffic if most mobile nodes are focused in a specific sector of the plane, the communications related to those nodes are enqueued until the beam is allowed in the specific sector; as a consequence, the larger the quantum assigned to each sector is, the larger the waiting queue time is. In the same way, as observed in [24], if the quantum assigned to each sector is too low, the system will provide bad performance in terms of overall throughput; a similar behavior is produced if the quantum assigned to each sector is averaged in a specific interval as the number of sectors increases, which results in the highest waiting queue time values.

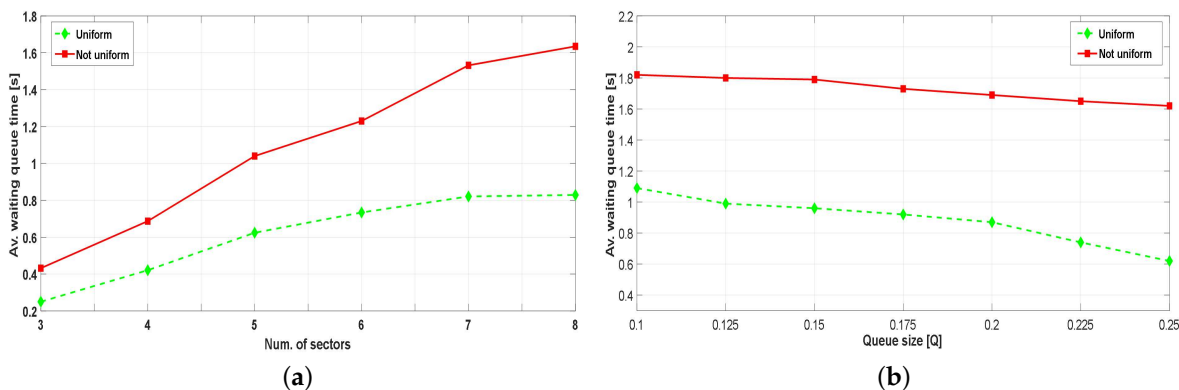


Figure 5. Queue issues with round-robin scheduling. (a) Average waiting queue time vs. number of sectors. (b) Average waiting queue time vs. queue size.

4. The Proposed Model

4.1. Comparison with RR-MAC and Motivations

In order to explain the relevance of using a round-robin based scheduling algorithm for directional MAC protocols let us consider the beamforming scenario shown in Figure 2a in which the round-robin approach is applied together with the plane sectorization of Figure 3. This process can be modeled as a Markov chain (Figure 6) defined by the following parameters:

- **state:** the set of the directions associated with a sector (in other terms, a state is a sector);
- **transition:** the switching process from a sector to another sector.

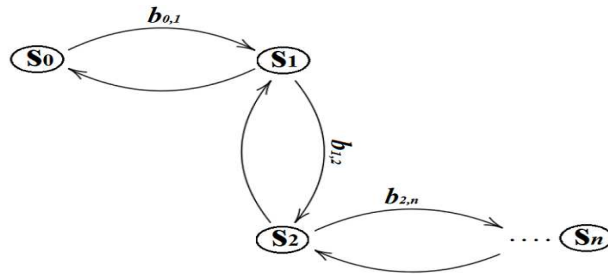


Figure 6. RR-MAC Markov model.

The transitions can be expressed as

$$b_{i,k} = \frac{T_i - k}{T_i} b_{i,0}, \quad 0 \leq i \leq N_s, \quad k \in [0, T_i]. \tag{3}$$

In Equation (3), $b_{i,0}$ represents the transition from the state i to the state 0; T_i is the duration of the sector i (sector time), while N_s is the maximum number of sectors. Figure 3 illustrates the Markov model applied to our case study. Assuming a beamforming context, considering a period T with $0 \leq T \leq T_i$, we make the following definitions:

- P_{sec} = prob. that a node x attempts for a transmission in a randomly chosen sector. $P_{sec} = 2/(T_i + 1)$
- P_{tr} = prob. that there is at least a transmission in a certain sector. $P_{tr} = 1 - (1 - P_{sec})^{N_s}$
- P_{nb} = prob. that at least one of the neighbors of x attempts for a transmission. $P_{nb} = (N_s - 1)(1 - P_{tr})$
- P_B = prob. that x is beamformed from at least one of its neighbors. $P_B = (1/N_s) + w(T_i)$

The term P_B depends on the number of sectors and on a weight assigned to each sector w ; in the case of the RR-MAC, for example, the weight is the same for each sector. We can express the probability that the node x experiences a collision in the considered period as follows:

$$P_c = P_B(T_i)P_{tr}(N_s - 1)P_{nb}(1 - P_{nb})^{N_s - 1}. \tag{4}$$

Note that P_B is a function of the sector time that also represents the beamforming time. As is clear from Equation (4), the larger the beamforming time is, the higher the number of frame collisions becomes. However, limiting the beamforming time of nodes is not a sufficient adjustment if the objective is to design an energy-efficient directional MAC approach. As explained in Section 3, the main challenges related to the RR-MAC approach are referred to the size of the queues and to the delay produced by static time slices that cannot be modeled in function of the traffic in the network. However, as observed in [23,24], the quantum of time assigned for the beamforming process is the same for each sector as well as the amplitude of the width. Therefore, in the work [24], a proper set of the sector time value affects the overall performance more than the sector width choice; this implies that the time slot assigned to sectors needs to be carefully assigned in order to improve system efficiency. For these reasons, we propose an approach that modifies the original round-robin algorithm formulation relative to the evaluation of the sector time, while keeping unchanged the sectorization of the plane and thus the width of the sectors. In order to understand the modifications introduced with respect to the round-robin MAC algorithm, we briefly recall the mathematical formulation of this latter:

$$\begin{aligned} \alpha_i &= \alpha_j = \dots = \alpha \\ T_i &= T_j = \dots = T_s \\ \alpha_i(T_i) &= \alpha_j(T_j) = \dots = \alpha(T) \\ \forall i, j &= 1, 2, \dots, N_s, \quad i \neq j. \end{aligned} \tag{5}$$

From the formulation given by Equation (5), it is easy to observe that the width is equal for all sectors as well as the sector time. The use of this approach helps to enhance the MAC performance in

terms of reduction of collisions and fairness improving, resulting in an overall decrease in the total amount of energy wasted by nodes. Unfortunately, RR-MAC is a static model and does not adapt itself to the traffic channel conditions; this could represent a limit in scenarios in which nodes are concentrated in a certain sector, as verified in the previous section. The goal of the present work is to improve the efficiency of the round-robin scheduler in terms of energy management by providing an adaptive beamforming time for each sector that takes into account the size of the waiting queue for each sector. We denoted this novel approach as adaptive beamforming time with round-robin MAC (ABT-RRMAC). To figure out the relevance of using an adaptive sector time assignment, let us consider the situation discussed in Section 3 in which two different mobile nodes traffic distribution (uniform and not uniform) in the network are compared:

Figure 7a represents a network scenario in which mobile nodes are almost uniformly distributed among sectors of the sectorized plane; the communications are ruled by the round-robin scheduling; therefore, the current active sector is Sector 2, and the beam is then active in that sector. As noticed from the analysis accomplished in Section 3, assuming a uniform activity degree of nodes, in this case, the waiting queue time is acceptable, as is the MAC layer performance; in Figure 7b, it can be observed that the overall node distribution is unbalanced among sectors as well as the activity degree of nodes. More specifically, most of the mobile nodes are mainly distributed in Sector 1, which, as an assumption, also has the highest activity degree among sectors; supposing that the current active sector is again Sector 2, which contains a very low number of nodes (compared to Sector 1) together with a very low burden of active communications, the allocated resources in that sector may be under-used; in particular, due to the static sector time reservation assignment provided by the round-robin algorithm (the assigned sector time is the same for all sectors), the overall beamforming process becomes inefficient, resulting in a considerable decreasing of the MAC performance especially in terms of throughput and energy consumption. Indeed, in Figure 7b, it is easy to observe that, due to unbalanced disposition of nodes among sectors, the energy consumption in sectors $S_2, S_3, S_4, S_5, S_7, S_8$ (representing the 80% of the overall plane) is quite inefficient because the beam, in that sector, is performed for a time T_s that is much higher than the required quantum of time required for emptying the queues. It is important to highlight that, because we are analyzing the worst condition case, we assume that the scenarios illustrated in Figure 7b remain unchanged for a long time or change very slowly.

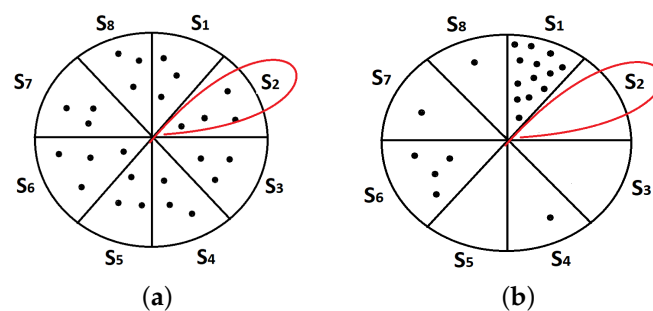


Figure 7. Uniform node distribution vs. non-uniform using round-robin approach. (a) Uniform node distribution. (b) Non-uniform node distribution.

4.2. ABT-RRMAC Formulation

In light of the previous considerations, our ABT-RRMAC approach modifies the original round-robin algorithm formulation regarding the evaluation of the sector time without affecting the plane sectorization and thus the width of the sectors. Basically, the idea is to assign a portion of time for each sector that is proportional to the size of the queues, that in this case is not fixed for each sector and can vary dynamically.

In Figure 8, an example of the ABT-RRMAC application is shown. The plane is normally sectorized into equalamplitude sectors as well as the round-robin MAC. However, in this case, we consider a traffic pattern that is not uniformly distributed among nodes; in Figure 8, it is assumed that, two particular sectors denoted S_x and S_y , respectively, have different sizes of frame waiting queues; in this regard, the term $size_{q_i}$ denotes the size of the waiting queue related to the i -th sector. While considering the situation in Figure 8, assuming that T_x and T_y are the beamforming (sector) times related to the sector x and y , respectively, the ABT-RRMAC assigns the beamforming times as follows:

$$\left\{ \begin{array}{l} T_1 = \frac{size_{q_1}}{\sum_{i=1}^N size_{q_i}} \times \bar{T} \neq T_s \\ \dots \\ \dots \\ T_N = \frac{size_{q_N}}{\sum_{i=1}^N size_{q_i}} \times \bar{T} \end{array} \right. \Rightarrow T_1 \neq T_2 \neq \dots \neq T_N \iff size_{q_1} \neq size_{q_2} \neq \dots \neq size_{q_N}$$

where

$$\bar{T} = \sum_{i=1}^N \frac{T_i}{N}. \tag{6}$$

The term \bar{T} denotes the mean beamforming time averaged by all sectors. Initially, the beamforming times are the same for all sectors and set to T_s (RR-MAC); after a training phase set to 10 s (the time of convergence of the RR-MAC), the mean beamforming time and then the sector times are updated periodically so that each sector is assigned a quantum of time that is proportional to the size of the queue of that sector multiplied by the mean beamforming time. In this way, sector times can be different and unbalanced, and the major fraction of time is assigned to the sector having the biggest queue size. For instance, if we consider the example of Figure 7, because $size_{q_x} > size_{q_y}$, the ABT-RRMAC will assign sector times such that $T_x > T_y$. The motivation of this choice is, due to the fact that $size_{q_x} > size_{q_y}$, the serving queue rate of S_x is lower than the serving queue rate of S_y ; consequently, S_x needs a beamforming time higher than S_y in order to empty its queue. Among other things, this choice will optimize the energy consumption of nodes in the network; in fact, the undesired waste of energy caused by the classic round-robin due to the static model is limited by the dynamic beamforming time assignment.

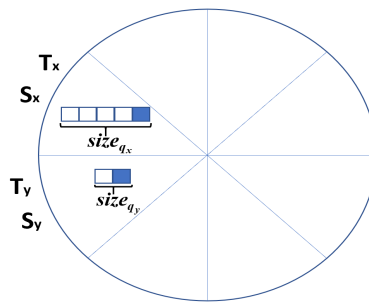


Figure 8. Adaptive beamforming time RR-MAC example.

4.3. ABT-RRMAC Implementation

The ABT-RRMAC algorithm is implemented in the Omnet++ network simulator in the *DcfUpperMAC* module, which is the main class in which the most important operations at the MAC layer are provided, such as frame and collision management; therefore, as explained in [24], the sectorization of the plane is managed by the SAS antenna module (*PhasedArray* module). The following pseudo-code (Algorithm 1) enhances the original round-robin MAC formulation:

Algorithm 1 ABT-RRMAC pseudo-code

```

1: procedure INIT(numSectors)
2:   numQueues  $\leftarrow$  numSectors
3:   CREATEQUEUES(numQueues)
4: end procedure

1: procedure ASSIGNSECTORTIME(trainingPeriod, updatePeriod, numQueues)
2:   if Sim.Time() < trainingPeriod || Sim.Time() < updatePeriod then
3:     averageSectorsTime = 0;
4:     for i = 1; i < numQueues; i++ do
5:       sectorTime[i] =  $T_s$ ;
6:     end for
7:   else
8:     averageSectorsTime = computeAverageSectorsTime()
9:     for i = 1; i < numQueues; i++ do
10:      sectorTime[i] =  $\frac{size_{q_i}}{\sum_{i=1}^N size_{q_i}} \times averageSectorsTime$ ;
11:    end for
12:   end if
13: end procedure

1: procedure STARTTRANSMIT(frame)
2:   int frameSector = getFrameSector(frame);
3:   int currentActiveSector = getCurrentActiveSector();
4:   if currentActiveSector != frameSector then
5:     queueSector[frameSector].insert(frame) // queue the frame
6:   else
7:     transmissionQueue.insert(frame);
8:     transmitFrame  $\leftarrow$  queueSector[activeSector].front()
9:     queueSector[activeSector].pop()
10:    CONFIGUREANTENNA(activeSector)
11:   end if
12: end procedure

1: procedure STARTRECEPTIONSTATE
2:   CONFIGUREANTENNA(omnidirectional)
3:   MAC in reception Mode
4:   SCHEDULEEVENT(CSMATimer)
5: end procedure

1: procedure RECEPTIONFRAME(frame)
2:   orientation  $\leftarrow$  GETORIENTATION(frame)
3:   sector  $\leftarrow$  GETSECTOR(orientation)
4:   CONFIGUREANTENNA(sector)
5: end procedure

1: procedure RECEIVEFRAMEFROMUPPERLAYERS(frame)
2:   sector  $\leftarrow$  GETSECTORFRAME(frame)
3:   queueSector[sector].push_back(frame)
4: end procedure

1: procedure MACPROCESS
2:   INIT(NumSectors)
3:   STARTRECEPTIONSTATE
4:   loop
5:     WaitEvent
6:     if Event Is Upper Frame then
7:       RECEIVEFRAMEFROMUPPERLAYERS(frame)
8:     else if Event Is Lower Frame then
9:       RECEPTIONFRAME(frame)
10:    else if End Transmission then
11:      STARTRECEPTIONSTATE
12:    else if EndCSMA  $\wedge$  QueueSector  $\neq$  empty then
13:      STARTTRANSMIT(frame)
14:    else
15:      STARTRECEPTIONSTATE
16:    end if
17:   end loop
18: end procedure

```

At the beginning of the process, after the plane is sectorized into equal width sectors, the same quantum of time is assigned for all sectors (round-robin). If the *trainingPeriod* has elapsed, the *averageSectorsTime* denoting the mean beamforming time averaged by all sectors can be computed; remember that this parameter is updated periodically after an *updatePeriod* (that we set to 10 s) has passed; from the first time that the *averageSectorsTime* is computed, the beamforming times of the sectors are assigned according to expressions defined in Section 4.2. The whole of these operations are included in the *AssignSectorTime* function. The transmission of frames is ruled by the *StartTransmit* function in which the system checks if the sector for which is destined the current frame is the *current active sector*. If true, it inserts the frame in the transmission queue and transmits the frame; otherwise, the frame is queued in its waiting sector queue and delayed until its sector is no longer the current active sector. The reception of the frame is performed by the *ReceptionFrame* and *ReceiveFromUpperLayers* functions in which the receiver antenna is configured in omnidirectional mode and the information about the orientation of the transmitter antenna is retrieved in order to achieve synchronization during the communication process. Other coordination functions are performed by the *MacProcess* procedure. The complexity of the algorithm can be evaluated by considering the *assignSectorTime* procedure because it includes most of the overall operations; in this case, because the sector time is computed and updated periodically for each sector, since we denoted with N_s the total number of sectors of the plane, it can be derived that the complexity is $O(N_s)$ in the best, in the medium, and in the worst cases; in poor terms, the complexity of ABT-RRMAC increases linearly with the number of sectors and not with the number of nodes. This is one of the benefits implied by the sectorized approach.

5. Performance Evaluation

In order to evaluate the contribution of the ABT-RRMAC, we perform simulations by considering three different configurations of antennas in the nodes: omnidirectional with round-robin scheduling, SASs with round-robin (RR-MAC), and our proposed ABT-RRMAC that uses SAS adaptive array antennas. Simulations are accomplished by varying the number of sectors and then the node mobility speed. The following table summarizes the main simulation parameters.

Simulations have been accomplished by using 20 different seeds and extracting the confidence intervals obtained by the repetitions considering a confidence level set to 95%. The traffic is represented by the UDP (user datagram protocol) data packets randomly generated (based on the simulation seed) by different couples of nodes. The number of nodes is set to 50 and couples of nodes involved in the data traffic exchange is one half with respect to the total number of nodes in the network. In addition, the channel is moderately affected from noise (-80 dBm), with SASs that have the main beam toward 45° . For the first set of simulations, we consider an unbalanced distribution of data (worst conditions) traffic by concentrating on the main fraction of communications in the first sector of the plane; therefore, nodes move very slowly (2 mps) in the network and the size of the queues is set to 5. The first evaluated statistic is the energy consumption of nodes by varying the number of sectors.

The plots in Figure 9 illustrate the energy consumption of nodes (expressed in Joules) in the function of the number of sectors (observe that the term "*N. Sector*" used in plots of Figure 9 is related to the progressive number ID assigned to each sector and does not identify N_s). In Figure 9a, it can be observed how the main fraction of consumption is related to Sector 1, the sector in which the traffic is mostly focused with respect to others. When omnidirectional antennas and the round-robin scheduler are used, the distribution of energy consumption among sectors is very unbalanced; this trend is mainly due to the static time slot assigned by the scheduler, that, in this case, is the same of all sectors; this feature results in an inefficient distribution of the energy in the sectors. Consequently, the total energy consumption is considerable (almost 298 J). However, the same behavior is maintained in Figure 9b in which, when SAS modules are used, a better distribution of the consumed energy among sectors can be highlighted. In Figure 9c, it appears clear that, as the number of sectors increases, the maximum amount of consumed energy is reduced; in the case of omnidirectional antennas, the imbalance remains unchanged. However, the use of the SAS allows one to decrease considerably

the maximum energy amount that is further reduced when the ABT-RRMAC approach is employed (44.54 against 88.27 registered in the omnidirectional case). Finally, Figure 9d further emphasizes the impact of the proposed approach, flowing in an overall balancing of the energy consumption. In summary, the dynamic allocation of the beamforming time allows one, independently from the number of sectors, to optimize the distribution of the energy also leading to a reduction of the overall consumed energy; indeed the registered values of total consumed energy in the RR-MAC case in the function of the number of sectors are 248.33, 255.14, 250.91, and 272.32 J against values of 187.89, 216.26, 211.81, and 235.37 J registered when the ABT-RRMAC is used. For a further investigation, it is possible to evaluate the standard deviation (averaging values by sectors) of the energy consumption by increasing the number of sectors for all of the configurations:

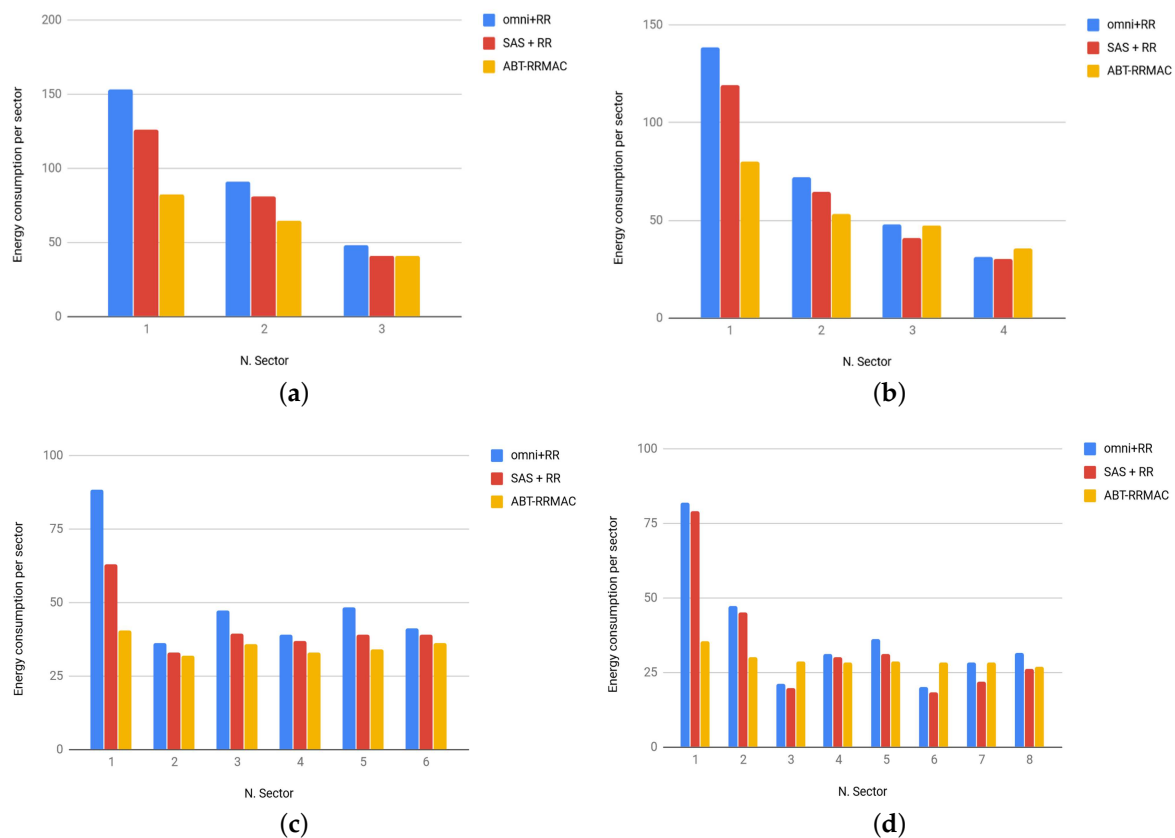


Figure 9. Energy consumption per sectors vs. number of sectors. (a) Energy consumption comparison, $N_s = 3$. (b) Energy consumption comparison, $N_s = 4$. (c) Energy consumption comparison, $N_s = 6$. (d) Energy consumption comparison, $N_s = 8$.

Table 2 collects standard deviation values by varying the number of sectors for all of the considered approaches; the use of the SAS slightly enhances the omnidirectional case; however, observe how ABT-RRMAC helps to dramatically decrease values when the number of sectors improves with respect to other considered configurations. This trend confirms that our proposed approach seeks to efficiently distribute the energy consumption among sectors as already noted in plots of Figure 9. Therefore, energy consumption is very related to packet delivery ratio (PDR) and could represent a helpful indication of the overall network performance; for this purpose, the next figure illustrates PDR comparison extracted by *rcvdPkts* and *sentPkts* statistics collected by Omnet++.

Table 2. Energy consumption: standard deviation vs. the number of sectors.

Number of Sectors	omni + RR	SAS + RR	ABT-RRMAC
3	52.96	42.79	20.55
4	47.02	39.6	19.03
6	19.04	20.69	3.03
8	18.71	18.15	2.62

In Figure 10, the average (averaged with respect to nodes) PDR is plotted both as a function of the number of sectors and the queue size. Figure 10a simply reflects the situation verified in Figure 9, in fact, the lower the energy consumption is, the higher the PDR; therefore, when the number of sectors is high, the ABT-RRMAC is able to provide a PDR of about 0.92 against 0.85 registered in the RR-MAC configuration. The same statistic can be evaluated by increasing the size of the queues; in Figure 10b (values are averaged with respect to number of sectors), it seems clear that PDR performance are quite sensitive to queue size, indeed, moderately. low values of PDR are obtained when omnidirectional antennas are used; SASs help to increase the minimum PDR from 0.62 to 0.72; however the minimum PDR value, when our proposed approach is used, is 0.84; this value slightly improves together with the queue size and tends to become almost uniform for the highest queue size values. More specifically, especially for critical queue size cases (from 3 to 5), the difference between RR-MAC and ABT-RRMAC is very significant; this result suggests that our proposed algorithm provides for a great robustness, even when the queue size is small, enabling an acceptable performance in the case of limited resource allocation. The latest set of simulations is accomplished with the aim to test our proposal under the condition of mobility of nodes; for this purpose, we evaluate the energy consumption of nodes by increasing the node mobility speed from 1 to 10 mps; in this case, results are obtained by averaging energy consumption values with respect to the number of sectors. In addition, we compared the worst queue size case (queue size = 3) and the best queue size case (queue size = 10).

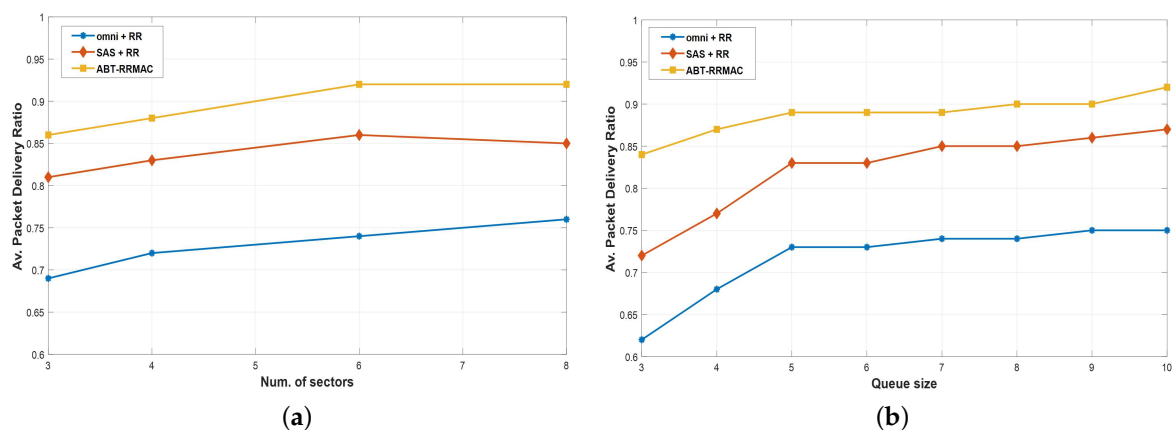


Figure 10. Packet delivery ratio (PDR) comparison. (a) Average PDR vs. number of sectors. (b) Average PDR vs. queue size.

Figure 11 displays comparison curves related to the energy consumption of nodes in the function of the mobility speed by considering the worst and the best registered case in the function of the size of the queues. Note that continued-line curves depict the worst case plots, while dashed-line curves are related to the best case plots. As regards the omnidirectional case, the overall consumption remains tolerant until 7 mps and then whereupon increases widely; this is mainly due to link failures occurring for high mobility speed values, which results in the enhancement of protocol overhead. However, this rapid increase is limited in the best omnidirectional case. When using an SAS in cooperation with round-robin, disruptive impacts due to the growth of node mobility speed are quite mitigated with respect to the omnidirectional case, especially for high mobility values. Therefore, the effects of

directional high-gain beamforming are quite straightforward; in particular, by considering the best and worst cases, the energy saving amount in the case of RR-MAC is from 23 to 29 J, compared to the omnidirectional case. Nevertheless, ABT-RRMAC, thanks to dynamic sector time assignment, improves the performance of the RR-MAC, extending battery life of nodes by about 21% (on average) compared to the latter. This effect seems to remain uniform as the mobility speed of nodes increases. Note that, when ABT-RRMAC curves related to the best and worst case are almost overlapped, indeed, the effect of queue size is mitigated compared to other considered cases.

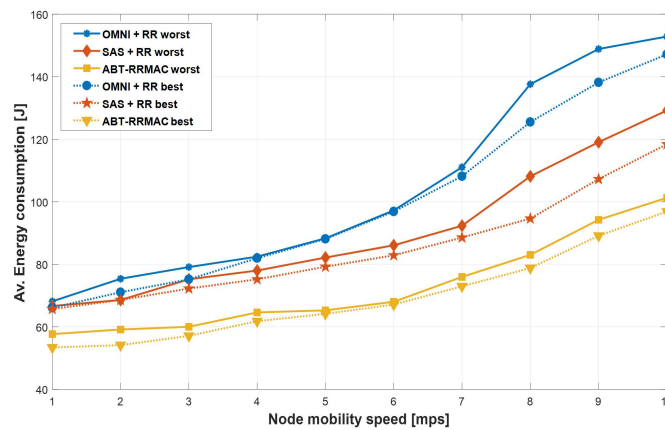


Figure 11. Energy consumption vs. node mobility speed.

6. ABT-RRMAC Comparison with DA-MAC

In order to estimate the contribution of ABT-RRMAC with respect to the current state of art, we chose to analyze and then to implement one of the most recent contributions cited in the related work section.

6.1. DA-MAC Implementation and Motivations

We decided to focus our attention on the DA-MAC protocol proposed in [26] for two main reasons:

1. Although the DA-MAC does not deal with a sectorized approach as well as our proposal, the work is extremely related with the deafness problem but does not consider the energy consumption of nodes.
2. Unlike the most of the cited related works that use the traditional directional antennas, DA-MAC establishes that the mobile nodes are equipped with a switched beam SAS technology. This feature is getting very close to our implementation model, which employs an SAS adaptive array.

The first step consists in the implementation of the DA-MAC on Omnet++. Basically, we slightly modify the *Dcf.cc* and *Contention.cc* modules provided by Omnet++ by inserting the DA-MAC algorithm designed in [26]. The *Dcf.cc* module controls the directional RTS/CTS exchange process and allows for channel access, while the *Contention.cc* module is essentially an FSM (finite state machine), which defines three possible node states: *Idle*, *Defer*, *IfsAndBackoff*; note that the *Defer* state coincides with the deaf state defined in the DA-MAC algorithm. The *Dcf* and the *Contention* modules communicate with each other through signals realizing together the MAC layer in the simulator. The DA-MAC algorithm provides for a partitioning of the single MAC channel into two channels (control channel and data channel); however, the IEEE802.11 standard does not cover the possibility of separating channels inside the same MAC; for this reason, we decide to use the *Multimac* code provided by Omnet++: in this regard, the two independent channels are emulated by using two different MAC interfaces: one for data traffic and one for control packets.

6.2. Performance Evaluation

The simulations of the DA-MAC are accomplished in Omnet++ by using the switched beam SAS module that we designed in [46]. The number of antenna elements of the array is set to 10; because DA-MAC does not allow for a plane sectorization, the overall MAC performance of the considered approaches are evaluated in function of the number of mobile nodes in the network; the number of nodes are increased from 10 to 100. The first statistic is referred to the PDR.

Figure 12 illustrates the comparison plot of the considered approaches related to the PDR statistic. When the number of nodes is low, the DA-MAC performs quite similarly to the ABT-RRMAC. Indeed, as demonstrated in [26], the peak of DA-MAC is obtained for a number of nodes set to 20; however, this value, for DA-MAC, tends to linearly decrease when the number of nodes is higher than 50; the average reduction changes from 4 to 12%; This is probably closely related to the different kinds of SAS technology used by the two approaches; in fact, the higher the number of nodes is, the higher the correlation matrix associated to the network is, and the lower the accuracy in the DOA (direction of arrival) estimation is; more specifically, the adaptive SAS technology used in ABT-RRMAC, due to its complex and efficient logical processing unit, is able to reduce the overall error introduced by the direction estimation better than the switched beam technology; once again, it is easy to observe how the gain introduced by ABT-RRMAC against RR-MAC in terms of PDR is considerable. For a further investigation, the energy consumption of the considered approaches varying the number of nodes has been analyzed.

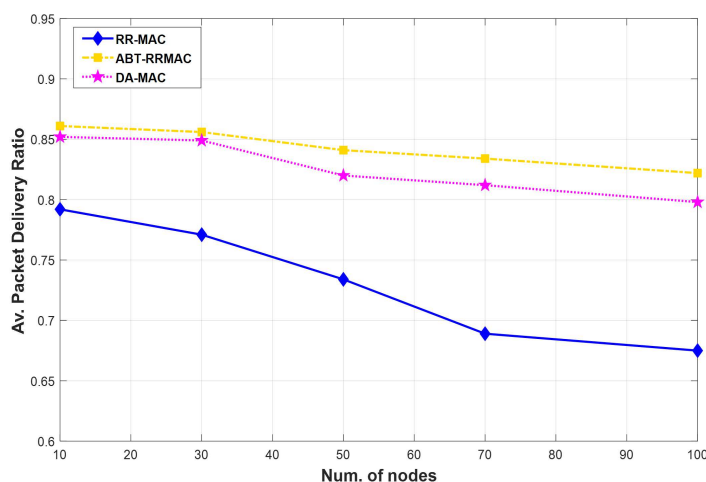


Figure 12. PDR-considered approaches.

The trend of curves plotted in Figure 13 is consistent with the results of Figure 12. In particular, ABT-RRMAC and DA-MAC operate very similarly with a small number of nodes. As the number of nodes enhances, DA-MAC energy consumption increases considerably and reaches a value of 85.13 J against the 75.16 obtained by ABT-RRMAC in the worst case. This behavior is probably motivated by the fact that the DA-MAC algorithm tends to reinforce the basic backoff procedure provided by classical directional MAC (which is the same used by ABT-RRMAC) increasing the number of retransmissions in the case of collision; as a consequence, the highest number of retransmissions of DA-MAC with respect to ABT-RRMAC translates into the highest energy consumption of DA-MAC compared to our proposal. Finally, based on considerations given in Section 4.3, it is possible to further justify the obtained results. Indeed, in the case of DA-MAC, the overall complexity of the algorithm can be assumed to be $O(N)$, namely it is linear with the number of nodes because the loop operation is performed by all nodes in the network. This translates into a higher number of operations of the DA-MAC with respect to ABT-RRMAC and then into a higher energy consumption.

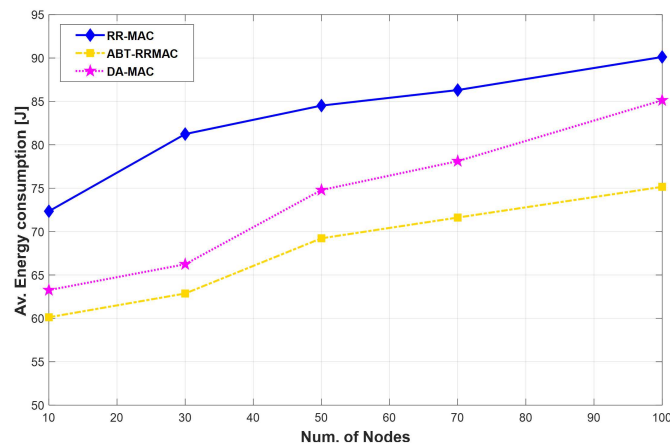


Figure 13. Energy consumption.

7. Conclusions

We proposed an adaptive beamforming time with round-robin MAC approach with the goal to improve benefits in terms of energy consumption introduced by the employment of round-robin scheduling in directional antenna MANET contexts [24]. This work has been mainly motivated by the fact that, although a round-robin approach is able to counteract main directional antenna issues that can usually occur at the MAC layer, the energy consumption distribution is not well distributed among sectors. Basically, the unbalanced energy distribution, due to problems introduced by round-robin such as the time slice and queue issues, promotes a non-negligible waste of energy that can limit the overall network performance, especially in terms of packet delivery ratio. In order to attempt to mitigate these problems, we proposed a solution that aims to eliminate the static assignment of the beamforming (or sector) time for sectors that could bring about a non-efficient energy distribution among sectors. The presented solution provides a dynamic assignment of the beamforming time by considering the current size of the sector queues and the average beamforming time; all parameters are updated periodically. The main advantage of that dynamic assignment is that, when data traffic is unbalanced in the simulation scenario, the slower a certain sector is to empty its queue (that is directly related to the size of the queue), the higher the quantum of time assigned to that sector is. The ABT-RRMAC has been compared to the classic omnidirectional MAC exploiting the round-robin principle and with the RR-MAC presented in [23,24] that uses SASs instead of omnidirectional antennas. Results, in terms of the energy consumption of nodes, by considering different configuration cases related to the number of sectors, show how ABT-RRMAC is able to reduce the maximum energy consumption amount per sector by about 37% on average, with respect to RR-MAC, and even 50% compared with the omnidirectional case. Furthermore, our proposed approach helps to level the energy consumption of nodes by uniformly distributing the total amount among sectors. For a further investigation, the PDR of all considered cases was evaluated as a function of the number of sectors and queue size; with reference to queue size, ABT-RRMAC provides for a minimum PDR of 0.84, which considerably improves the value of 0.72 obtained in RR-MAC. This result is significant because the dependency of the PDR is reduced with queue size. Finally, our approach has been evaluated in terms of energy consumption by considering the mobility of nodes; in this regard, results show that ABT-RRMAC outperforms RR-MAC; this trend remains almost uniform independently from the size of the queues. Lastly, in order to evaluate our contribution with respect to the current state of the art, we implemented and analyzed the DA-MAC protocol and compared it with our proposal. Results show that DA-MAC is quite similar to ABT-RRMAC in terms of PDR if the number of nodes in the network is limited; our protocol tends to outperform DA-MAC as the number of nodes increases. The same trend is reflected with regard to the energy consumption of nodes in which a difference in terms of wasted energy occurs between DA-MAC and our proposed approach; in this respect, ABT-RRMAC preserves more energy compared to DA-MAC mainly because of the relatively small number of operations performed.

The Table 3 summarizes the list of symbols used in the manuscript:

Table 3. List of symbols used in this manuscript.

Symbol	Explanation
Q	term referred to the queue size
N	number of nodes
N_s	number of sectors
w_Q	queue weight
\overline{W}_Q	queue weight vector
S_i	i-th sector
T_i	i-th sector time
T_s	sector time
α_i	i-th sector angle
$size_{q_i}$	i-th sector queue size
\overline{T}	mean beamforming time
λ	wavelength
s	seconds
m	meters
mps	meters per seconds
J	joules
dBm	decibel-milliwatts

Author Contributions: V.I. contributed to most of the formulations and simulations and implemented the proposed model under the supervision of F.D.R. and A.A.Q.; A.F.S. was responsible for data curation and results validation and helped revise the paper.

Funding: This research received no external funding

Conflicts of Interest: The authors declare no conflict of interest.

Abbreviations

The following abbreviations are used in this manuscript:

SASs	smart antenna systems
MAC	medium access control
OMNI	omnidirectional
DMAC	directional medium access control
RR-MAC	round-robin MAC
ABT-RRMAC	adaptive beamforming round-robin medium access control
DA-MAC	deafness-aware medium access control
MANET	mobile ad hoc network
VANET	vehicular ad hoc network
SDMA	spatial division multiple access
DRTS	directional request to send
DCTS	directional clear to send
DNAV	directional network allocator vector
CPU	central Processing Unit
SRL	short Retry Limit
PDR	packet delivery ratio
AODV	ad hoc on demand distance vector

References

1. Dai, H.; Kam-Wing, N.G.; Min-You, W. An overview of MAC protocols with directional antennas in wireless ad hoc networks. In Proceedings of the International Conference Wireless and Mobile Communications (ICWMC), Bucharest, Romania, 29–31 July 2006.
2. Huang, Z.; Chien-Chung, S. A comparison study of omnidirectional and directional MAC protocols for ad hoc networks. In Proceedings of the Global Telecommunications Conference (GLOBECOM), Taipei, Taiwan, 17–21 November 2002.
3. Choudhury, R.R.; Vaidya, N.H. Deafness: A MAC problem in ad hoc networks when using directional antennas. In Proceedings of the IEEE International Conference on Network Protocols (ICNP), Berlin, Germany, 8 October 2004; pp. 283–292.
4. Cassano, E.; Florio, F.; De Rango, F.; Marano, S. A performance comparison between ROC-RSSI and trilateration localization techniques for WPAN sensor networks in a real outdoor testbed. In Proceedings of the Wireless Telecommunications Symposium (WTS), Prague, Czech Republic, 22–24 April 2009; pp. 1–8.
5. Arrawatia, M.; Baghini, M.S.; Kumar, G. Broadband bent triangular omnidirectional antenna for RF energy harvesting. *IEEE Antennas Wirel. Propag. Lett.* **2016**, *15*, 36–39. [[CrossRef](#)]
6. Li, B.; Xue, Q. Polarization-reconfigurable omnidirectional antenna combining dipole and loop radiators. *IEEE Antennas Wirel. Propag. Lett.* **2016**, *12*, 1102–1105. [[CrossRef](#)]
7. Gustafsson, M.; Sohl, C.; Kristensson, G. Physical limitations on antennas of arbitrary shape. *Proc. R. Soc. Lond. A* **2007**, *463*, 2589–2607. [[CrossRef](#)]
8. De Rango, F.; Gerla, M.; Marano, S. A scalable routing scheme with group motion support in large and dense wireless ad hoc networks. *Comput. Electr. Eng.* **2006**, *32*, 224–240. [[CrossRef](#)]
9. Dai, H.; Ng, K.; Li, M.; Wu, M. An overview of using directional antennas in wireless networks. *Int. J. Commun. Syst.* **2013**, *26*, 413–448. [[CrossRef](#)]
10. Suhag, S.; Gupta, A.; Duhan, M. Improvement of QoS Parameters by using Directional Antennas in MANET. *Int. J.* **2016**, *5*, 1026–1031.
11. Kumari, N.; Kumar, R.; Bajaj, R. Energy Efficient Communication Using Reconfigurable Directional Antenna in MANET. *Procedia Comput. Sci.* **2018**, *125*, 194–200. [[CrossRef](#)]
12. Kumari, N.; Kumar, R.; Bajaj, R. Mobile ad hoc networks and energy efficiency using directional antennas: A Review. In Proceedings of the International Conference on Intelligent Computing and Control Systems (ICICCS), Madurai, India, 15–16 June 2017; pp. 1213–1219.
13. Jiang, D.; Xu, Z.; Li, W.; Chen, Z. Network coding-based energy-efficient multicast routing algorithm for multi-hop wireless networks. *J. Syst. Softw.* **2015**, *104*, 152–165. [[CrossRef](#)]
14. Patra, S.; Pandey, A.; Nandni, N.; Kumar, S.; Jha, V.; Kumar, M. Power pattern synthesis of smart antenna array using different adaptive algorithms. *Int. J. Adv. Res.* **2015**, *3*, 1459–1466.
15. He, C.; Liang, X.; Zhou, B.; Geng, J.; Jin, R. Space-division multiple access based on time-modulated array. *IEEE Antennas Wirel. Propag. Lett.* **2015**, *14*, 610–613. [[CrossRef](#)]
16. Niu, J.; Zhang, R.; Cai, L.; Yuan, J. A Fully-Distributed MAC Protocol for Mobile Ad Hoc Networks. In Proceedings of the International Conference on Communications (ICC), London, UK, 8–12 June 2015.
17. Wang, G.; Xiao, P.; Li, W. A novel MAC protocol for wireless network using multi-beam directional antennas. In Proceedings of the International Conference on Computing, Networking and Communications (ICCNC), Santa Clara, CA, USA, 26–29 January 2017.
18. Wang, J.; Ren, X.; Chen, F.J.; Chen, Y.; Xu, G. On MAC optimization for large-scale wireless sensor network. *Wirel. Netw.* **2016**, *22*, 1877–1889. [[CrossRef](#)]
19. Zhou, B.; Lee, Y.Z.; Gerla, M.; De Rango, F. Geo-LANMAR: A scalable routing protocol for ad hoc networks with group motion. *Wirel. Commun. Mob. Comput.* **2006**, *6*, 982–1002. [[CrossRef](#)]
20. Jones, C.; Sivalingam, K.; Agrawal, P.; Chen, J. Survey of energy efficient network protocols for wireless networks. *Wirel. Netw.* **2001**, *7*, 343–358. [[CrossRef](#)]
21. Chou, J.; Petrovic, D.; Ramchandran, K. A distributed and adaptive signal processing approach to reduce energy consumption in sensor networks. In Proceedings of the Twenty-second Annual Joint Conference of the IEEE Computer and Communications Societies, San Francisco, CA, USA, 30 March–3 April 2003.
22. Swaminathan, A.; Noneaker, D.L.; Russell, H.B. The design of a channel-access protocol for a wireless ad hoc network with sectored directional antennas. *Ad Hoc Netw.* **2012**, *10*, 284–298. [[CrossRef](#)]

23. Inzillo, V.; De Rango, F.; Quintana, A.A. A sectorized directional MAC proposal for mitigating deafness and energy consumption in mobile ad hoc networks. In Proceedings of the 15th Consumer Communications and Networking Conference (CCNC), Las Vegas, NV, USA, 12–15 January 2018; pp. 1–2.
24. Inzillo, V.; De Rango, F.; Santamaria, A.F.; Quintana, A.A. A round-robin MAC approach for limiting deafness in mobile ad hoc network beamforming environments. In Proceedings of the Wireless Days Conference (WD), Dubai, UAE, 3–5 April 2018; pp. 98–100.
25. Wei, Y.; Heidemann, J.; Estrin, D. An energy-efficient MAC protocol for wireless sensor networks. In Proceedings of the Twenty-First Annual Joint Conference of the IEEE Computer and Communications Societies, New York, NY, USA, 23–27 June 2002.
26. Na, W.; Park, L.; Cho, S. Deafness-aware MAC protocol for directional antennas in wireless ad hoc networks. *Ad Hoc Netw.* **2015**, *24*, 121–134. [[CrossRef](#)]
27. Sivalingam, K.; Chen, J.; Agrawal, P.; Strivastava, M. Design and analysis of low-power access protocols for wireless and mobile ATM networks. *Wirel. Netw.* **2001**, *6*, 73–87. [[CrossRef](#)]
28. Gossain, H.; Cordeiro, C.; Cavalcanti, D.; Agrawal, D. The deafness problems and solutions in wireless ad hoc networks using directional antennas. In Proceedings of the Global Telecommunications Conference Workshops (GLOBECOM), Dallas, TX, USA, 29 November–3 December 2004; pp. 108–113.
29. Huang, P.; Xiao, X.; Soltani, S. The evolution of MAC protocols in wireless sensor networks: A survey. *IEEE Commun. Surv. Tutor.* **2013**, *15*, 101–120. [[CrossRef](#)]
30. Huang, Z.; Chen, Y.; Li, C. PSR: A lightweight proactive source routing protocol for mobile ad hoc networks. *IEEE Trans. Veh. Technol.* **2014**, *63*, 859–868.
31. Haider, M.; Knightly, M. Mobility resilience and overhead constrained adaptation in directional 60 GHz WLANs: Protocol design and system implementation. In Proceedings of the 17th International Symposium on Mobile Ad Hoc Networking and Computing (ISCC), Paderborn, Germany, 5–8 July 2016.
32. Chen, J.; Sivalingam, K.; Agrawal, P.; Acharya, R. Scheduling multimedia services in a low-power MAC for wireless and mobile ATM networks. *IEEE Trans. Multimed.* **1999**, *1*, 187–201. [[CrossRef](#)]
33. De la Chapelle, M.; Monk, A. Soft Handoff Method and Apparatus for Mobile Vehicles Using Directional Antennas. U.S. Patent 7555299, 5 April 2016.
34. Lu, X.; Lio, P.; Hui, P.; Jin, H. A Location Prediction Algorithm for Mobile Communications Using Directional Antennas. *Int. J. Distrib. Sens. Netw.* **2013**, *4*, 1–10. [[CrossRef](#)]
35. Inzillo, V.; De Rango, F.; Quintana, A.A.; Zampogna, L. Mobility Beamforming Prediction and a Round Robin Scheduling in a Directional MAC for MANET. In Proceedings of the Wireless and Mobile Networking Conference (WMNC), Prague, Czech Republic, 3–5 September 2018.
36. Everett, E.; Sahai, A.; Sabharwal, A. Passive self-interference suppression for full-duplex infrastructure nodes. *IEEE Trans. Wirel. Commun.* **2014**, *13*, 680–694. [[CrossRef](#)]
37. Korakis, T.; Jakllari, G.; Tassiulas, L. A protocol for full exploitation of directional antennas in ad hoc wireless networks. *IEEE Trans. Mob. Comput.* **2008**, *1*, 145–155. [[CrossRef](#)]
38. Li, Y.; Safwat, A. On wireless ad hoc networks with directional antennas: Efficient collision and deafness avoidance mechanisms. *EURASIP J. Wirel. Commun. Netw.* **2008**, *7*, 867–882. [[CrossRef](#)]
39. Divecha, B.; Abraham, A.; Grosan, C.; Sanyal, S. Impact of node mobility on MANET routing protocols models. *J. Digit. Inf. Manag. (JDIM)* **2007**, *5*, 19–23.
40. Lenders, V.; Wagner, J.; May, M. Analyzing the impact of mobility in ad hoc networks. In Proceedings of the 2nd International Workshop On Multi-Hop Ad Hoc Networks: From Theory to Reality, Florence, Italy, 26 May 2006.
41. Omnet++ Simulator, Vers. 5.2. 2018. Available online: www.omnetpp.org (accessed on 13 February 2018).
42. Inzillo, V.; De Rango, F.; Quintana, A.A. A Low Energy Consumption Smart Antenna Adaptive Array System For Mobile Ad Hoc Networks. *Int. J. Comput.* **2017**, *16*, 124–132.
43. Abdullah, A.A.; Cai, L.; Gebali, F. DSDMAC: Dual sensing directional MAC protocol for ad hoc networks with directional antennas. *IEEE Trans. Veh. Technol.* **2012**, *61*, 1266–1275. [[CrossRef](#)]
44. Jha, J.; Chowdhury, S.; Ramya, G. Survey on various scheduling algorithms. *Imp. J. Interdiscip. Res.* **2017**, *3*, 1749–1752.

45. Fataniya, B.; Patel, M. Survey on different method to improve performance of the round robin scheduling algorithm. *Int. J. Res. Sci. Eng. Technol.* **2018**, *6*, 69–77.
46. Inzillo, V.; De Rango, F.; Santamaria, A.F.; Quintana, A.A. A new switched beam smart antenna model for supporting asymmetrical communications extending Inet Omnet++ framework. In Proceedings of the Performance Evaluation of Computer and Telecommunication Systems International Symposium (SPECTS), Seattle, WA, USA, 9–12 July 2017; pp. 1–7.



© 2018 by the authors. Licensee MDPI, Basel, Switzerland. This article is an open access article distributed under the terms and conditions of the Creative Commons Attribution (CC BY) license (<http://creativecommons.org/licenses/by/4.0/>).